International Journal for Multidisciplinary Research (IJFMR)
E-ISSN: 2582-2160 ● Website: www.ijfmr.com ● Email: editor@ijfmr.com

Coordinated OLTC–Volt/VAR Control for Voltage Regulation and Curtailment Reduction in PV Integrated Distribution Networks

Dhaval Yogeshbhai Raval[1], Saurabh N. Pandya[2]

[1]Ph.D Scholar, Gujarat Technological University, Chandkheda, Ahmedabad, Gujarat, India.
[2]Professor, Department of Electrical Engineering, Vishwakarma Engineering College, Chandkheda, Ahmedabad, Gujarat, India.

ABSTRACT
The growing integration of rooftop photovoltaic (PV) systems in low-voltage distribution networks poses challenges for maintaining voltage quality, minimizing curtailment, and reducing stress on network assets. This study evaluates and compares three voltage regulation strategies: brute-force optimization-based on-load tap changer (OLTC) control, conventional Volt/VAR with active power curtailment, and a coordinated OLTC–Volt/VAR control scheme. The coordinated approach, which prioritizes global voltage centering through OLTC before engaging inverter-based Volt/VAR support, demonstrates superior performance across multiple indicators. It enhances voltage stability, reduces the frequency of tap operations, and improves PV utilization by lowering the need for curtailment. These results highlight the coordinated OLTC–Volt/VAR control as a practical and effective solution for enabling higher PV penetration while maintaining reliable and efficient distribution system operation.

Keywords: Photovoltaic, Distribution Network, Voltage Rise, OLTC, Volt/VAR

1. Introduction

The transformation of electric power distribution systems is being driven by the rapid integration of distributed energy resources (DERs)—particularly photovoltaic (PV) generation—into medium and low voltage feeders [1]. This decentralization presents significant operational challenges for traditional voltage regulation mechanisms, which were originally designed for unidirectional power flows and relatively predictable load profiles [2],[3]. One of the most concerning issues in this modern distribution network is voltage rise under high PV penetration, where fast, localized voltage excursions can occur due to the intermittent nature of solar generation and the absence of sufficient controllable loads [4],[5].

Maintaining voltage within statutory limits is critical for both equipment protection and power quality assurance. However, traditional voltage regulation tools such as On-Load Tap Changers (OLTCs)—which adjust the transformer tap position to regulate downstream voltages—are ill-equipped to manage the dynamic and localized voltage variations characteristic of high PV scenarios [6]. OLTCs are typically operated under a centralized control paradigm and suffer from mechanical constraints, including limited tap resolution and wear-related degradation, which restrict the frequency of operation. Consequently, while OLTCs are effective for slow, feeder-wide voltage regulation, they are insufficient for addressing fast and spatially distributed fluctuations caused by cloud-induced PV variability or rapid changes in localized demand [7].

In contrast, smart inverters equipped with Volt/VAR control capabilities can respond within seconds to local voltage conditions by adjusting their reactive power output based on pre-programmed droop characteristics [8]. This distributed and fast-reacting control modality enables inverters to provide fine-grained voltage support in real time. However, this benefit comes at a cost. Reactive power support is limited by the inverter's apparent power rating, and prioritizing reactive power can lead to real power curtailment, thereby reducing PV utilization and the associated economic returns [9]. Moreover, when reactive power demands approach the inverter's capacity, aggressive Volt/VAR control can result in significant energy losses and suboptimal operation.

Recent literature has increasingly recognized the need for coordinated voltage control strategies that leverage the strengths of both OLTCs and smart inverters while mitigating their respective limitations. In such hybrid schemes, the OLTC performs slow and global voltage cantering, while the inverters provide fast, local correction to handle finer deviations. Several studies have explored co-optimization frameworks and distributed control algorithms to achieve this coordination [10]–[12]. However, challenges remain in the design of computationally efficient, scalable, and real-time capable control strategies that can be implemented within the constraints of existing infrastructure.

To address these challenges, this paper proposes a coordinated OLTC–Volt/VAR control strategy tailored for real-time deployment in high PV penetration feeders. The approach consists of two sequential control layers:

1. A brute-force OLTC tap selection mechanism that exhaustively searches over a discrete set of tap positions to minimize a global voltage cantering objective function.
2. A Volt/VAR droop-based inverter control scheme with active power curtailment, where inverters inject or absorb reactive power according to their local voltage measurements.

This design reduce the burden on inverters, minimizing real power curtailment, and limiting excessive mechanical wear on the OLTC through the use of incremental tap movements and smoothing mechanisms.

The remainder of the paper is structured as follows: Section 2 presents the detailed control algorithms for OLTC tap selection and inverter-based Volt/VAR control. Section 3 describes the simulation study and performance metrics. Section 4 discusses the results and comparative analysis.

2. Modified IEEE 906 Bus LV Distribution Network

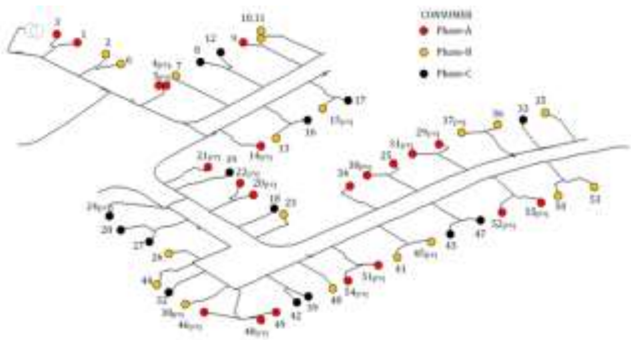

Figure 1 Modified IEEE 906 Bus LV Distribution Network

Figure 1 illustrates the IEEE 906-Bus Low Voltage (LV) Distribution Network, which includes a total of 55 consumers distributed across Phase A, Phase B, and Phase C. Since the study focuses on single-phase rooftop photovoltaic (PV) systems, the analysis is limited to Phase A of the network.

To simulate PV integration, the test feeder was modified by assigning PV systems to selected consumers. The allocation strategy is based on individual consumer load demand — consumers with higher energy consumption are prioritized for PV installation, as they offer better potential for self-consumption and load matching.

Table.1 presents the load characteristics (maximum, minimum, and average demand in kW) for Phase A consumers, along with the PV assignment, which is marked by an asterisk (*) next to the consumer number.

Table 1 Consumer load demand analysis

Consumer Number	Max (kW)	Min (kW)	Average (kW)
1	2.771	0.036	0.426
3*	8.308	0.054	0.2842
4	5.180	0.048	0.409
5	3.438	0.035	0.2895
9*	6.840	0.059	0.8063
14	2.471	0.049	0.2246
20*	6.223	0.051	0.5417
21	3.067	0.045	0.2200
22	1.833	0.054	0.2040
25	3.320	0.050	0.2790
29*	10.549	0.054	0.5234
30	3.044	0.053	0.2837
31*	8.297	0.053	0.2888
34*	8.566	0.045	0.2508
46*	7.844	0.049	0.4001
48*	8.894	0.046	0.4460
49	3.485	0.054	0.3344
51	3.566	0.053	0.3459
52*	8.267	0.052	0.2437
54	3.299	0.048	0.3919
55	2.901	0.055	0.3003

2. Impact of PV Integration on the Voltage Profile of Consumers

Table 2 Impact of PV Integration

Consumer Number	Before PV integration		After PV Integration		
	V_{min}	V_{max}	V_{min}	V_{max}	Duration $V > 6\%$ (Minute)
1	0.9886	1.0033	0.9905	1.0281	0

Consumer Number	Before PV integration		After PV Integration		
	V_{min}	V_{max}	V_{min}	V_{max}	Duration $V > 6\%$ (Minute)
3	0.9875	1.0034	0.9905	1.0291	0
4	0.9832	1.0097	0.9820	1.0578	0
5	0.9835	1.0097	0.9823	1.0575	0
9	0.9785	1.0125	0.9773	1.0717	34
14	0.9799	1.0139	0.9779	1.0737	55
20	0.9732	1.0179	0.9719	1.0955	148
21	0.9751	1.0166	0.9738	1.0864	107
22	0.9735	1.0219	0.9722	1.0949	145
25	0.9653	1.0218	0.9684	1.1172	191
29	0.9584	1.0227	0.9693	1.1262	208
30	0.9653	1.0218	0.9687	1.1172	191
31	0.96	1.0227	0.9693	1.1259	207
34	0.9677	1.0211	0.9698	1.1165	191
46	0.9636	1.0192	0.9666	1.1072	181
48	0.9653	1.019	0.9658	1.1067	180
49	0.9633	1.0191	0.9663	1.1063	179
51	0.9654	1.0203	0.9688	1.1041	176
52	0.964	1.0215	0.9681	1.1129	192
54	0.9656	1.0203	0.9690	1.1041	176
55	0.9653	1.0215	0.9678	1.1117	191

The integration of rooftop photovoltaic (PV) systems has a significant impact on the voltage profile of low-voltage distribution networks as shown in Table.2. Table.2 compares the minimum and maximum voltages observed at various consumer nodes before and after PV integration in Phase A of the IEEE 906-Bus LV Distribution Network. A general increase in voltage, particularly in the maximum voltage (V_{max}), is evident across nearly all PV-integrated consumers. The most notable voltage rise is observed at Consumer 29, where V_{max} increased from 1.0227 p.u. to 1.1262 p.u., representing a maximum voltage rise of approximately 10.1%. On average, the increase in maximum voltage across PV-integrated nodes is around 7.6%, indicating a clear trend of voltage elevation due to localized power injection by PV units.
Furthermore, the clustering of PV installations—where multiple consumers are assigned PV in close proximity—intensifies this effect. Nodes such as Consumers 25, 29, 30, 31, and 34, which are spatially close, exhibit sustained over-voltage events. This clustering effect causes cumulative voltage rise, not only affecting the PV hosting consumers but also impacting neighbouring non-PV consumers. For example, Consumer 22, a non-PV node adjacent to several PV consumers, shows a post-integration V_{max} of 1.0949 p.u., up from 1.0219 p.u., indicating that voltage rise can propagate downstream or upstream depending on network topology.
The duration of over-voltage—measured as time duration for which voltage exceeds 6% above nominal—is also a critical metric. Consumers like 29, 31, and 52 experience over-voltage durations exceeding 190

minutes, which can degrade equipment lifespan, disrupt protection settings, and violate voltage quality standards (e.g., IEEE 1547, IEC 61000).

3. Voltage Regulation Approach

The preceding analysis clearly demonstrates that high PV penetration, particularly when clustered, can lead to significant voltage rise and extended over-voltage durations within the distribution network. These voltage excursions, if not mitigated, can compromise power quality, violate regulatory limits, and pose risks to both utility infrastructure and customer equipment. Therefore, robust voltage regulation mechanisms are essential to ensure network stability.

To address these challenges, this section proposes two complementary control strategies aimed at mitigating over-voltage conditions in high-PV environments: (1) Brute-force optimization-based OLTC tap selection, which operates at the system level to centrally adjust voltage levels via transformer tap settings, and (2) Volt/VAR control with active power curtailment, a decentralized approach that leverages inverter capabilities at the local level.

3.1 Brute Force Optimization based OLTC Tap Selection

The on-load tap changer (OLTC) is a widely used device for voltage control at the substation level. It adjusts the transformer turns ratio to regulate the secondary voltage and maintain it within acceptable limits across downstream customers.

Among various control strategies, the brute-force optimization approach offers a simple yet effective method for OLTC tap selection. Unlike heuristic or model-based methods, brute-force optimization evaluates all possible tap positions within the allowable range and selects the one that minimizes a voltage deviation objective function.

At each decision instant t, a fixed set S of customer nodes is monitored. Their single-phase line-to-neutral voltages are converted to per-unit (p.u.) values using a common voltage base $V_{\text{base}} = 240$ V. The per-unit voltage measurement for customer i at time t is given by:

$$v_i(t) = \frac{V_i^{\text{mag}}(t)}{V_{\text{base}}} \dots\dots\dots..(1)$$

The action of the OLTC is modeled by proportional scaling of all downstream voltages. For a candidate tap ratio τ, the predicted per-unit voltage at customer i becomes:

$$\hat{v}_i(t;\tau) \approx \tau v_i(t) \dots\dots\dots(2)$$

The OLTC operates over a discrete set of admissible tap ratios T, bounded by mechanical limits and spaced uniformly. For instance, tap positions ranging from 0.90 to 1.10 p.u. in increments of $\Delta\tau = 0.00625$ p.u. form the set:

$$T = \{\tau_{\min}, \tau_{\min} + \Delta\tau, \dots, \tau_{\max}\} \dots\dots\dots(3)$$

For each candidate tap ratio $\tau \in T$, the algorithm evaluates a centering objective function $J(\tau)$, defined as the sum of absolute deviations of customer voltages from 1 p.u.:

$$J(\tau) = \sum_{i \in S} |\hat{v}_i(t;\tau) - 1| = \sum_{i \in S} |\tau v_i(t) - 1| \dots\dots\dots(3)$$

Finally, the optimal tap ratio $\tau^*(t)$ to be applied at time t is the one that minimizes the objective:

$$\tau^*(t) \in \arg\min_{\tau \in T} J(\tau) \dots\dots\dots(4)$$

This brute-force strategy ensures that the voltage profile across the monitored nodes is kept as close as possible to the nominal 1 p.u. value, enhancing voltage quality and network stability under varying PV generation conditions.

3.2 Volt/VAR Control with Active Power Curtailment

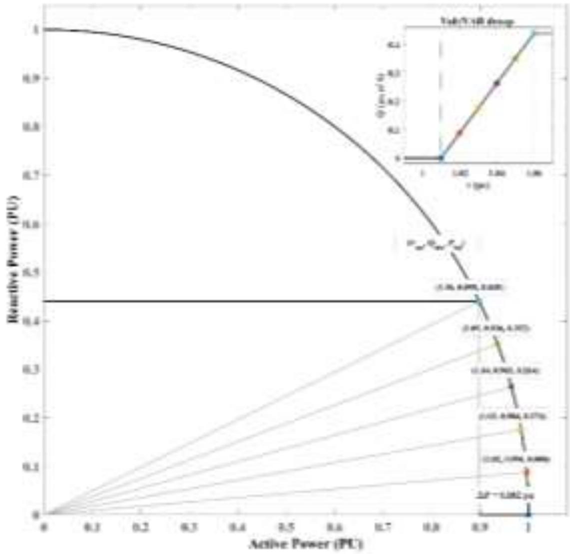

Figure 2 Volt/VAR Control with Active Power Curtailment

This control approach is based on a Volt/VAR droop characteristic shown in Figure.2 which relates terminal per-unit voltage to the reactive power setpoint of the inverter. When the voltage rises above the upper deadband, the inverter absorbs inductive VARs, and when it falls below the lower deadband it injects capacitive VARs, while within the deadband it provides nearly zero reactive power. The requested reactive power $Q^{\star}$ is then subject to two limits: the study-defined $Q_{max} \leq \kappa_Q S_{\max}$ and the inverter's kVA circle constraint $P^2 + Q^2 \leq S_{\max}^2$.

$$k = \begin{cases} +1, & V_{\text{pu}} \leq 0.94, \\ \dfrac{0.99 - V_{\text{pu}}}{0.05}, & 0.94 < V_{\text{pu}} < 0.99, \\ 0, & 0.99 \leq V_{\text{pu}} \leq 1.01, \\ \dfrac{1.06 - V_{\text{pu}}}{0.05} - 1, & 1.01 < V_{\text{pu}} < 1.06, \\ -1, & V_{\text{pu}} \geq 1.06. \end{cases} \ldots\ldots\ldots (5)$$

$$Q^{*} = kQ_{max} \ldots\ldots\ldots (6)$$

To ensure feasibility, the available active power is curtailed whenever necessary according to

$$P^{\star} = \min\left(P_{\text{avail}}, \sqrt{S_{\max}^2 - (Q^{\star})^2}\right) \ldots\ldots\ldots (7)$$

so that the reactive demand is always satisfied (VAR-priority) and the inverter operates strictly within its nameplate. The figure illustrates this principle: the inset shows the four-point Volt/VAR droop curve, while the main plot maps the resulting (P, Q) operating points on the capability circle. As voltage increases (e.g., from 1.02 pu to 1.06 pu), progressively larger reactive absorption is commanded, and the corresponding maximum permissible active power reduces, visible as the shift from the upper-right edge toward the interior of the circle. The difference between the available and the dispatched real power represents curtailed energy, here amounting to $\Delta P = 0.102$pu at the most extreme case. In this way, the inverter supports feeder voltage regulation by prioritizing reactive power injection or absorption, with minimal but controlled sacrifice of real power output.

4. Coordinated Voltage Regulation Approach

4.1 Need for Coordinated Control

Individually, both OLTC and Volt/VAR controls contribute to voltage regulation, but each has clear limitations. The OLTC is a centralized and relatively slow device, constrained by mechanical wear and restricted tap movements, which limits its responsiveness to rapid fluctuations from distributed PV generation. In contrast, inverter-based Volt/VAR control is fast and distributed, capable of reacting within seconds at local nodes, but its operation can force significant active power curtailment whenever reactive demands approach the kVA limit. If applied in isolation, OLTC control may fail to contain fast voltage excursions, while Volt/VAR control alone may lead to unnecessary energy losses and reduced PV utilization. These complementary disadvantages highlight the need for coordinated control, wherein the OLTC provides slower, system-level centering of voltages while inverters handle fast, local deviations, thereby minimizing both excessive tap operations and PV curtailment.

4.2 Coordinated OLTC–Volt/VAR Control Strategy

At each decision instant, node voltages $v_i(t)$ from equation - (1) are used to select the OLTC tap first via the brute force search over the discrete set of equation - (3), evaluating the centering objective given in equation - (4) and choosing $\tau^{\star}$ by equation -(5). A small smoothing increment (your $DT = 0.05/16$) is applied to avoid chatter before writing the tap on the secondary winding, followed by a power-flow solve. This global, slow, centralised action recentres feeder voltages, reducing the need for large local VARs in the subsequent step and limiting mechanical operations via incremental tap movement.

With the feeder re-solved at the new tap, all inverters then act locally and fast using the same minute's measurements: each unit resets to curtailed $P_{\text{mpp},0}$, solves to obtain P_{avail} and V_{pu}, computes the Volt/VAR request from the droop map given in equation - (6) capped by $Q_{\max}$ using equation - (7), and enforces feasibility on the capability circle through the VAR-priority real-power limit in equation-(8). This tap-first ordering ensures the OLTC performs the broad voltage centering so that most nodes fall inside the droop deadband (hence $Q^{\star} \approx 0$), while the inverters provide only residual, nodal correction; as a result, voltage compliance is achieved with fewer tap operations than fully local control and with less PV curtailment than inverter-only operation-yet maintains responsiveness to fast PV/load fluctuations within each minute cycle.

5. Result & Discussion

Across the 21 consumers, the box-plot distributions in Figure.3 and the consumer-wise extremes in Table.3 indicate that the Coordinated Control (autotransformer centering with PV Volt/VAR limited to $|Q| \leq 0.44$ p.u.) provides the most favorable voltage behavior, with OLTC alone performing second, and Volt/VAR with curtailment performing least well on several indicators. At the fleet level, the typical operating point remains close to nominal for the transformer-based strategies (median of medians ≈ 1.007 p.u. for both Coordinated and OLTC), whereas Volt/VAR alone operates at a higher center (≈ 1.018 p.u.). Dispersion is smallest under the coordinated scheme (median IQR ≈ 0.0246 p.u), slightly larger for OLTC (0.0264 p.u.), and substantially larger for Volt/VAR (0.0421 p.u.). The proportion of time within the tight $0.99 - 1.01$ p.u. band follows the same ordering: $\approx 42\%$ for Coordinated and OLTC versus $\approx 27\%$ for Volt/VAR. Tail metrics also favor the coordinated approach: the fleet-median Q_{95} is ≈ 1.041 p.u. (OLTC:

1.046 ; Volt/VAR: 1.073) and the fleet-median daily maximum is ≈ 1.052 p.u. (OLTC: 1.059; Volt/VAR: 1.084). Continuity of excursions is markedly reduced when the autotransformer is active: the median longest continuous run above 1.01 p.u. is ∼ 1.6 h for Coordinated and OLTC, compared with ∼ 7.3 h for Volt/VAR. Consistently, the median time above 1.05 p.u. is ≈ 0.017 h with Coordinated, 0.40 h with OLTC, and 2.87 h with Volt/VAR. These distributional results are achieved without inducing under-voltage; minimum values under the transformer-based strategies remain within the 0.95 p.u. envelope (lowest around 0.960 − 0.966 p.u. in the table).

The node-wise extremes and durations substantiate these fleet-level trends. Summed across all consumers, the cumulative time with $v > 1.06$ p.u. decreases from 2752 min in the baseline PV network to 1928 min with Volt/VAR, 220 min with OLTC, and 61 min with the coordinated scheme; the number of affected consumers drops from 17/21 (baseline) to 15/21 (Volt/VAR), 10/21 (OLTC), and 5/21 (Coordinated). Heavily stressed nodes benefit most when the autotransformer recenters the

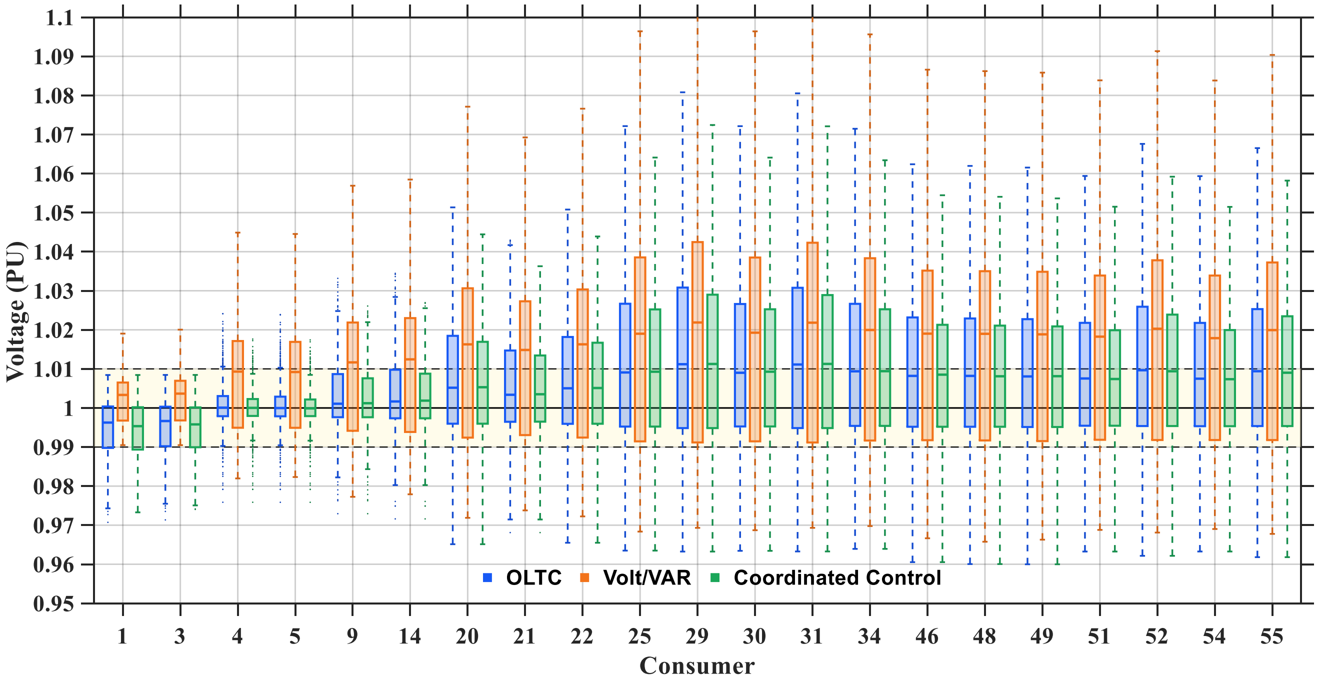

Figure 3 Box Plot Representation of Consumer Voltage Profile

Table 3 Consumer-Wise Extremes

Consumer Number	**PV Integrated Distribution Network**			**Volt/VAR with PV Curtailment**			**Brute Force Optimization Based Tap Changer Control**			**Coordinated Control**		
	V_{min}	V_{max}	$V > 6\%$ (Min)	V_{min}	V_{max}	$V > 6\%$ (Min)	V_{min}	V_{max}	$V > 6\%$ (Min)	V_{min}	V_{max}	$V > 6\%$ (Min)
1	0.9905	1.0281	0	0.9905	1.0190	0	0.9707	1.0084	0	0.9733	1.0084	0

Consumer Number	PV Integrated Distribution Network			Volt/VAR with PV Curtailment			Brute Force Optimization Based Tap Changer Control			Coordinated Control		
	V_{min}	V_{max}	$V > 6\%$ (Min)	V_{min}	V_{max}	$V > 6\%$ (Min)	V_{min}	V_{max}	$V > 6\%$ (Min)	V_{min}	V_{max}	$V > 6\%$ (Min)
3	0.9905	1.0291	0	0.9905	1.0200	0	0.9714	1.0085	0	0.9740	1.0085	0
4	0.9820	1.0578	0	0.9820	1.0449	0	0.9759	1.0241	0	0.9759	1.0176	0
5	0.9823	1.0575	0	0.9823	1.0445	0	0.9759	1.0239	0	0.9759	1.0174	0
9	0.9773	1.0717	34	0.9773	1.0569	0	0.9729	1.0332	0	0.9729	1.0261	0
14	0.9779	1.0737	55	0.9779	1.0585	0	0.9716	1.0345	0	0.9716	1.0270	0
20	0.9719	1.0955	148	0.9719	1.0771	87	0.9651	1.0513	0	0.9651	1.0444	0
21	0.9738	1.0864	107	0.9738	1.0692	40	0.9681	1.0429	0	0.9681	1.0363	0
22	0.9722	1.0949	145	0.9722	1.0766	86	0.9655	1.0508	0	0.9655	1.0439	0
25	0.9684	1.1172	191	0.9684	1.0964	161	0.9635	1.0721	21	0.9635	1.0641	2
29	0.9693	1.1262	208	0.9693	1.1047	177	0.9632	1.0808	68	0.9632	1.0724	28
30	0.9687	1.1172	191	0.9687	1.0964	161	0.9634	1.0721	21	0.9634	1.0641	2
31	0.9693	1.1259	207	0.9693	1.1043	177	0.9633	1.0805	67	0.9633	1.0721	27
34	0.9698	1.1165	191	0.9698	1.0956	161	0.9639	1.0715	21	0.9639	1.0634	2
46	0.9666	1.1072	181	0.9666	1.0866	125	0.9605	1.0624	1	0.9605	1.0544	0
48	0.9658	1.1067	180	0.9658	1.0862	120	0.9600	1.0620	1	0.9600	1.0540	0
49	0.9663	1.1063	179	0.9663	1.0858	120	0.9600	1.0615	1	0.9600	1.0536	0
51	0.9688	1.1041	176	0.9688	1.0839	114	0.9633	1.0594	0	0.9633	1.0515	0

Consumer Number	**PV Integrated Distribution Network**			**Volt/VAR with PV Curtailment**			**Brute Force Optimization Based Tap Changer Control**			**Coordinated Control**		
	V_{min}	V_{max}	$V > 6\%$ (Min)	V_{min}	V_{max}	$V > 6\%$ (Min)	V_{min}	V_{max}	$V > 6\%$ (Min)	V_{min}	V_{max}	$V > 6\%$ (Min)
52	0.968	1.112	192	0.968	1.091	146	0.962	1.067	12	0.962	1.059	0
54	0.969	1.104	176	0.969	1.083	114	0.963	1.059	0	0.963	1.051	0
55	0.967	1.111	191	0.967	1.090	139	0.961	1.066	7	0.961	1.058	0

feeder and PVs provide only residual correction: Consumers 25 and 34 reduce > 1.06 exposures from 191 to 2 minutes; Consumers 29 and 31 reduce from 208/207 to 28/27 minutes; and Consumers 20-22 eliminate all > 1.06 events (to 0 minutes), while their maxima retreat from $\approx 1.095 - 1.126$ p.u. to $\approx 1.044 - 1.072$ p.u. In contrast, Volt/VAR alone yields only partial relief at these sites (e.g., Consumer 29: 208 → 177 minutes with maxima remaining > 1.10 p.u.), which is consistent with its higher center, wider IQR, and longer high-voltage runs in the box-plots. At lightly stressed nodes (e.g., 1 and 3), all strategies satisfy limits with narrow, nominal-centered distributions. Overall, the combined evidence from the box-plots and the per-node table demonstrates that autotransformer-first coordination-together with Volt/VAR constrained to $|Q| \leq 0.44$ p.u. as needed-achieves the lowest peaks, the tightest spread, and the shortest high-voltage episodes across the feeder.

Table 4 Comparative Analysis of OLTC Operation

Parameter	**Brute Force Based OLTC Control**	**Coordinated Control**
Number of Tap Change throughout the day	85	63
Highest Tap Position (PU)	1.0125	1.0125
Lowest Tap Position (PU)	0.95	0.9562

The comparative analysis of the tap operation shown in Table.4 highlights the operational advantages of the proposed Coordinated OLTC–Volt/VAR Control strategy over the Brute Force Based OLTC Control. As observed, the coordinated control results in fewer tap changes (85) compared to the brute force method (63), indicating a reduction in mechanical wear and improved operational efficiency of the OLTC. Despite this reduction, the voltage regulation range is effectively maintained, with both strategies reaching the same maximum tap position of 1.0125 p.u., while the minimum tap position is slightly improved for the coordinated method (0.9562 p.u.) than for the brute force method (0.95 p.u.), reflecting a more conservative and smoother tap adjustment behavior.

The energy curtailment analysis presented in Figure. 5 provides a comparative assessment of the conventional Volt/VAR control with PV curtailment and the proposed Coordinated OLTC–Volt/VAR control strategy across ten distinct PV systems.

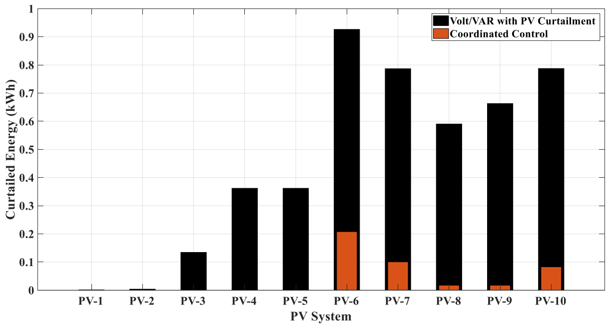

Figure 4 Energy Curtailment

Table 5 Reactive Power Injection & Active Power Curtailment

PV System	**Volt/VAR with PV Curtailment**		**Coordinated Control**		**Energy Saving**
	Q_{abs} (Max) **kVAR**	P_{inj} (Max) **kW**	Q_{abs} (Max) **kVAR**	P_{inj} (Max) **kW**	**kWh**
PV-1	1.478	7.711	0.000	7.712	0.0006
PV-2	2.315	4.820	0.684	4.820	0.0037
PV-3	4.379	8.648	2.019	8.676	0.1344
PV-4	3.032	5.778	2.591	5.784	0.3620
PV-5	3.032	5.778	2.591	5.784	0.3620
PV-6	4.249	7.725	4.005	7.763	0.7183
PV-7	4.183	7.717	3.940	7.756	0.6860
PV-8	3.600	6.747	3.390	6.751	0.5729
PV-9	4.111	7.705	3.872	7.712	0.6456
PV-10	4.150	7.703	3.909	7.738	0.7046

As observed, the coordinated approach significantly reduces the amount of curtailed energy in nearly all systems, demonstrating its effectiveness in improving PV utilization. In particular, systems such as PV-6, PV-10, and PV-9 show marked reductions in curtailed energy, with savings of 0.7183 kWh, 0.7046 kWh, and 0.6456 kWh, respectively, compared to the conventional method. This improvement is attributed to the tap-first coordination mechanism, wherein the OLTC performs global voltage centering, thereby ensuring that the majority of nodes remain within the Volt/VAR droop deadband. As a result, inverters are required to absorb significantly less reactive power, thereby minimizing the need to curtail active power. Furthermore, the reactive power absorption values Q_{abs} are consistently lower under coordinated control without compromising the real power injection capability of the PV units. For instance, PV-1 exhibits zero reactive power absorption under coordinated control, while still maintaining a slightly improved real power output. The aggregate energy savings across all PV systems over the 24-hour simulation period amount to 4.1902 kWh, underscoring the coordinated strategy's advantage in enhancing both voltage regulation and overall system energy efficiency. These findings confirm that coordinated control not only mitigates excessive mechanical tap operations, as discussed earlier, but also leads to tangible energy gains in high-PV penetration networks.

4. Conclusion

At the fleet level, the coordinated control maintained a median operating point close to nominal (≈1.007 p.u.) with the lowest voltage dispersion (median IQR ≈0.0246 p.u.), compared to larger deviations under OLTC-only and Volt/VAR strategies. Over-voltage mitigation was markedly improved, with cumulative time above 1.06 p.u. reduced from 2752 minutes in the baseline PV network to only 61 minutes under coordinated control. In addition, the number of affected consumers dropped from 17 of 21 in the baseline to just 5 under the coordinated scheme.

From an operational perspective, the coordinated method reduced OLTC tap operations to 751 compared to 790 under brute-force control, indicating lower mechanical wear without compromising voltage range. Energy curtailment was also significantly mitigated: individual PV systems achieved savings up to 0.7183 kWh, while the aggregate savings across all systems over 24 hours amounted to 4.1902 kWh. Overall, these findings confirm that Coordinated OLTC–Volt/VAR control is an effective and scalable solution for high-PV distribution networks.

References

1. Panda, S., Mohanty, S., Rout, P. K., Sahu, B. K., Parida, S. M., Kotb, H., & Shouran, M. An insight into the integration of distributed energy resources and energy storage systems with smart distribution networks using demand-side management. Appl. Sci. 12 (2022) 8914, doi: https://doi.org/10.3390/app12178914.
2. Shaukat, N., Islam, M. R., Rahman, M. M., Khan, B., Ullah, B., Ali, S. M., & Fekih, A. Decentralized, democratized, and decarbonized future electric power distribution grids: a survey on the paradigm shift from the conventional power system to micro grid structures. IEEE Access. 11 (2023) 60957-60987, doi: https://doi.org/10.1109/ACCESS.2023.3287628.
3. Putratama, M. A. Towards Decentralization of Voltage Management Strategies for Smart Distribution Systems: Application to Energy Communities. Doctoral dissertation, Université Grenoble Alpes, (2022).
4. Hamza, E. A., Sedhom, B. E., & Badran, E. A. Impact and assessment of the overvoltage mitigation methods in low-voltage distribution networks with excessive penetration of PV systems: A review. Int. Trans. Electr. Energ. Syst. 31 (2021) e13161, doi: https://doi.org/10.1002/2050-7038.13161.
5. Korab, R., Połomski, M., & Smołka, M. Evaluating the risk of exceeding the normal operating conditions of a low-voltage distribution network due to photovoltaic generation. Energies. 15 (2022) 1969, doi: https://doi.org/10.3390/en15061969.
6. Spertino, F., Ciocia, A., Mazza, A., Nobile, M., Russo, A., & Chicco, G. Voltage control in low voltage grids with independent operation of on-load tap changer and distributed photovoltaic inverters. Electr. Power Syst. Res. 211 (2022) 108187, doi: https://doi.org/10.1016/j.epsr.2022.108187.
7. Kabir, F., Gao, Y., & Yu, N. Reinforcement learning-based smart inverter control with polar action space in power distribution systems. In: Proc. 2021 IEEE Conf. Control Technol. Appl. (CCTA). IEEE, (2021) 315-322, doi: https://doi.org/10.1109/CCTA48906.2021.9659183.

8. Chathurangi, D., Jayatunga, U., Perera, S., Agalgaonkar, A. P., & Siyambalapitiya, T. Comparative evaluation of solar PV hosting capacity enhancement using Volt-VAr and Volt-Watt control strategies. Renew. Energy. 177 (2021) 1063-1075, doi: https://doi.org/10.1016/j.renene.2021.06.042.
9. Sharma, V., Haque, M. H., Aziz, S. M., & Kauschke, T. Reducing overvoltage-induced PV curtailment through reactive power support of battery and smart PV inverters. IEEE Access. (2024), doi: https://doi.org/10.1109/ACCESS.2024.XXXXX.
10. Singh, B., & Kumar Sharma, A. Impact of D-STATCOM and OLTC with integrated Volt/VAR control in distribution system for power loss minimization and voltage control. Smart Sci. 11 (2023) 334-354, doi: https://doi.org/10.1080/23080477.2023.2178423.
11. Xie, Y., Ding, Z., Ding, L., & Zhang, Q. Multi-objective Volt-Var Optimization Considering Operation Cost of OLTC in Distribution Networks. In: Proc. 2024 21st Int. Conf. Harmonics and Quality of Power (ICHQP). IEEE, (2024) 690-694, doi: https://doi.org/10.1109/ICHQP59906.2024.XXXXXXX.
12. Hou, Q., Dai, N., & Huang, Y. Voltage regulation enhanced hierarchical coordinated Volt/VAR and Volt/Watt control for active distribution networks with soft open points. IEEE Trans. Sustain. Energy. 15 (2024) 2021-2037, doi: https://doi.org/10.1109/TSTE.2024.3346237.